Available online at www.sciencedirect.com
ScienceDirect
Applied Catalysis B: Environmental 83 (2008) 229–239
APPLIED CATALYSIS B: ENVIRONMENTAL
www.elsevier.com/locate/apcatb

Effect of sintering on the catalytic activity of a Pt based catalyst for CO oxidation: Experiments and modeling

J. Yang [a], V. Tschamber [a,*], D. Habermacher [a], F. Garin [b], P. Gilot [a]

[a] Laboratoire Gestion des Risques Environnement, Université de Haute Alsace, 25 rue de Chemnitz, 68200 Mulhouse, France
[b] Laboratoire des Matériaux, Surfaces et Procédés pour la Catalyse, Ecole Européenne Chimie Polymères et Matériaux, 25 rue Becquerel, 67087 Strasbourg Cedex, France

Received 3 December 2007; received in revised form 4 February 2008; accepted 9 February 2008
Available online 26 February 2008

Abstract

The goal of this paper was to make the link between sintering of a 1.6% Pt/Al_2O_3 catalyst and its activity for CO oxidation reaction. Thermal aging of this catalyst for different durations ranging from 15 min to 16 h, at 600 and 700 °C, under 7% O_2, led to a shift of the platinum particle size distributions towards larger diameters, due to sintering. These distributions were studied by transmission electron microscopy. The number and the surface average diameters of platinum particles increase from 1.3 to 8.9 nm and 2.1 to 12.8 nm, respectively, after 16 h aging at 600 °C. The catalytic activity for CO oxidation under different CO and O_2 inlet concentrations decreases after aging the catalyst. The light-off temperature increased by 48 °C when the catalyst was aged for 16 h at 600 °C. The CO oxidation reaction is structure sensitive with a catalytic activity increasing with the platinum particle size. To account for this size effect, two intrinsic kinetic constants, related either to platinum atoms on planar faces or atoms on edges and corners were defined. A platinum site located on a planar face was found to be 2.5 more active than a platinum site on edges or corners, whatever the temperature. The global kinetic law $\{r\ (\text{mol m}^{-2}\ \text{s}^{-1}) = 103 \times \exp(-64{,}500/RT)[O_2]^{0.74}[CO]^{-0.5})\}$ related to a reaction occurring on a platinum atom located on planar faces allows a simulation of the CO conversion curves during a temperature ramp. Modeling of the catalytic CO conversion during a temperature ramp, using the different aged catalysts, allows prediction of the CO conversion curves over a wide range of experimental conditions.

Keywords: Carbon monoxide; Oxidation; Modeling; Sintering; Platinum based catalyst

1. Introduction

To achieve emission standards, automotive exhausts have to be treated. Catalytic converters are monoliths with channels coated with alumina in which noble metals are dispersed. The efficiency of the catalysts towards CO and hydrocarbons oxidation and NO reduction is dependent on the size of the catalyst particles in relation with the state of dispersion of the active metal [1]. This dispersion changes when the converter is exposed to alternatively oxidative and reductive atmospheres and to high temperature fluctuations (up to ~800 °C). After exposure for long periods at elevated temperatures, especially under oxidising conditions, sintering of the noble metals occurs and leads to a decrease in their catalytic activity [2,3]. The rate of sintering increases dramatically with temperature and becomes significant above 600 °C.

Since the early seventies, a large number of studies have investigated the phenomenon of sintering of Pt dispersed on various supports [1–5]. Thermal or thermo-chemical degradation, is probably the main cause for deactivation of catalysts. Thus, most of the studies are focused on the influence of temperature and time of exposure on growth of metal particles under oxidising atmosphere. Concerning Pt/Al_2O_3 catalysts, rapid sintering of platinum in an oxidising atmosphere occurs above 600 °C [6–9]. Ruckenstein and Malhotra [7] reported that under an oxidising atmosphere, for temperature below 550 °C, the dispersion is relatively insensitive to the duration of treatment, while at higher temperature, the dispersion after a 16 h (or a 128 h) aging treatment was significantly lower than after a 1 h treatment.

Few studies have analyzed the effect of the surrounding gas atmosphere at moderate and high temperatures [3,10,11]. Lööf

* Corresponding author. Tel.: +33 3 89 32 76 58; fax: +33 3 89 32 76 61.
E-mail address: valerie.tschamber@uha.fr (V. Tschamber).

0926-3373/$ – see front matter © 2008 Elsevier B.V. All rights reserved.
doi:10.1016/j.apcatb.2008.02.018

Nomenclature

a	constant ratio k_{plan}/k_{other}
d_i	diameter of particle i (m)
d_n	number average particle diameter (m)
d_s	surface average particle diameter (m)
D	metal dispersion (%)
D_T	volumetric flow rate ($m^3\ s^{-1}$)
f_{plan}	fraction of Pt atoms on planar faces
f_{other}	fraction of Pt atoms on edge and corner
F	total volumic flow ($m^3\ s^{-1}$)
k	kinetic constant ($mol^{0.77}\ m^{-1.31}\ s^{-1}$)
k_i	kinetic constant corresponding to a particle of diameter d_i ($mol^{0.77}\ m^{-1.31}\ s^{-1}$)
k_{plan}	intrinsic kinetic constant corresponding to planar faces atoms ($mol^{0.77}\ m^{-1.31}\ s^{-1}$)
k_{other}	kinetic constant corresponding to edge and corner atoms ($mol^{0.77}\ m^{-1.31}\ s^{-1}$)
m_{cata}	mass of the catalyst (kg)
m_{bed}	mass of the catalytic bed composed of the catalyst mixed in alumina (kg)
M_{Pt}	molar mass of Pt ($kg\ mol^{-1}$)
n_i	fraction of particles with a diameter d_i
r	reaction rate per surface unit of Pt particles ($mol\ m^{-2}\ s^{-1}$)
s_i	surface of particle with a diameter d_i (m^2)
S	section of the reactor (m^2)
T	temperature (°C)
v	local volumic reaction rate ($mol_{CO}\ m^{-3}\ s^{-1}$)
v_i	local volumic reaction rate of particles with a diameter i ($mol_{CO}\ m^{-3}\ s^{-1}$)
V	CO oxidation rate ($mol_{CO}\ s^{-1}$)
V_m	molar volume ($m^3\ mol^{-1}$)
X_{CO}	molar fraction of CO
X_{O_2}	molar fraction of O_2
z	axial coordinate (m)

Greek letters

α	reaction order with respect to O_2
β	reaction order with respect to CO
ρ_{Pt}	density of Pt ($kg\ m^{-3}$)
ρ_{bed}	density of the catalytic bed composed of the catalyst mixed in alumina ($kg\ m^{-3}$)
σ	area occupied by 1 mol of Pt at the surface ($m^2\ mol^{-1}$)
τ	CO conversion level (%)
τ_{Pt}	mass fraction of Pt (%)
$\tau_{Pt,i}$	mass fraction of Pt particles with a diameter d_i (%)

et al. [3] measured dispersion loss due to sintering of Pt in different atmospheres: oxidising (2% O_2 or 0.1–4% NO in Ar), reducing (4% H_2 or 4% CO) and neutral (Ar) at temperatures ranging from 200 to 700 °C. They showed that highly dispersed Pt clusters (1 nm diameter) on γ-Al_2O_3 are stable towards sintering in inert and reducing (H_2) atmospheres up to 700 °C. In contrast, oxidising atmospheres of O_2 or NO accelerate sintering. This is confirmed in the review on sintering by Wanke and Flynn [11] who pointed out that supported metal catalysts sinter faster under an oxidising atmosphere than under reducing and inert atmospheres. Mergler and Nieuwenhuys [12] have also suggested that well-dispersed catalysts are more sensitive to deactivation, in agreement with Granger et al. [13].

Particle size effects on the CO–O_2 oxidation rate, under stoichiometric reaction conditions, have been studied on supported metal catalysis [13–18]. The particle size seems to be a key factor which determines whether the CO oxidation reaction is structure sensitive, i.e., the intrinsic catalytic activity is dependent on the particle size, or not. It comes out that, for small metal particles (generally less than 2 nm) CO oxidation is structure sensitive [14,15,19] whatever the inlet CO/O_2 ratio and for larger particles the turnover frequency (TOF) is independent [20–25] or slightly dependent [26–27] on particle size under CO-rich or stoichiometric conditions.

In this study, a 1.6% Pt/Al_2O_3 catalyst was aged under 7% O_2/N_2 for different durations at temperature in the range 500–700 °C. Transmission electron microscopy (TEM) was used to study sintering of platinum in order to establish a correlation between the aging treatments and the sintering effect. Measurements of catalytic activity for CO oxidation under O_2 were performed for the different aged catalysts. The catalytic activity for CO oxidation was modeled, accounting for the change of the platinum surface area with the particle size distributions obtained by TEM. Structure sensitivity of the CO oxidation reaction was demonstrated. Hypotheses explaining this structure effect are proposed.

2. Experimental

2.1. Catalyst preparation

The Pt (1.6 wt%)/Al_2O_3 catalyst was prepared by wet impregnation of γ-alumina (Woehlm, 250 m^2/g) with a hexachloro platinic acid solution (Johnson Matthey, 38–40% Pt). After drying in air at 100 °C overnight, the catalyst was calcined at 500 °C for 2 h under an air flow (40 cm^3/min, standard conditions). Then, the catalyst was reduced under an H_2 flow (40 cm^3/min, standard conditions) at 360 °C for 2 h. The catalyst was sieved in the range 250–400 μm.

2.2. Catalytic activity for CO oxidation

The catalytic activity for CO oxidation was measured in a fixed bed quartz reactor (internal diameter 19 mm). The catalyst (200 mg) was mixed with 1800 mg of alumina. The temperature was measured by a thermocouple located within the bed of catalyst. Before experiment, the catalyst placed in the reactor was reduced at 500 °C for 1 h using 1% H_2 in nitrogen. Then, two types of experiments were performed. For experiments under a temperature ramp (10 K/min), the material was cooled to room temperature (hydrogen was switched to nitrogen at 100 °C). Subsequently, the CO/O_2 mixture in nitrogen was injected and the temperature program started. The

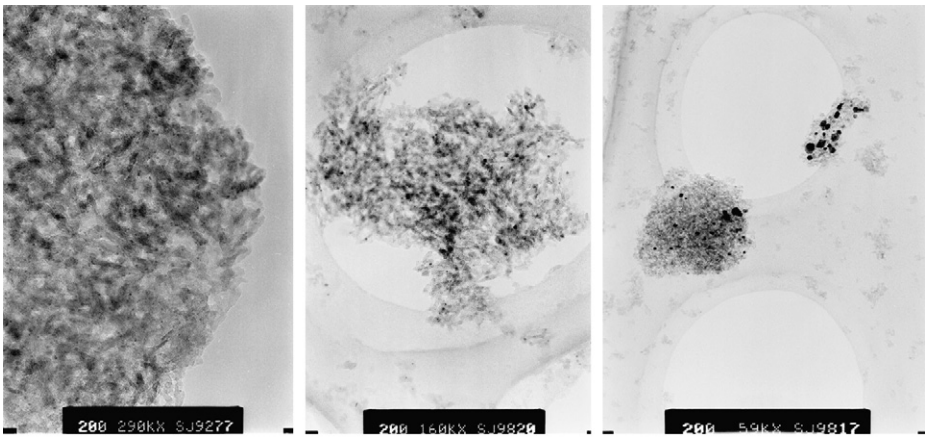

Fig. 1. Pictures obtained by TEM on a fresh catalyst (a) and after aging at 600 °C under 7% O_2 during 15 min (b) and 16 h (c).

total flow rate was 40 l h^{-1}, leading to a space velocity of 12,000 h^{-1}. For steady state isothermal experiments, the material was cooled up to the required temperature and then the CO/O_2 mixture in nitrogen was injected. These experiments were performed to estimate the CO oxidation order with respect to oxygen and CO. To estimate the reaction order with respect to oxygen, steady state isothermal (182.0 °C) CO oxidations were performed under a given inlet CO content (10,000 ppm) and different oxygen inlet contents ranging from 3000 to 10,000 ppm. To estimate the CO oxidation order with respect to CO, steady state isothermal (158.5 and 166.0 °C) CO oxidations were performed under a given inlet oxygen content (close to 2500 ppm) and different CO inlet contents ranging from 3000 to 7000 ppm. The reactor was used as a differential reactor since CO conversion was limited to a maximum of 15% in all cases.

The outlet gas was analyzed using an infrared ROSEMOUNT NGA 2000 analyzer to quantify outlet CO and CO_2 molar fractions.

2.3. Aging procedure

Catalyst aging was carried out with the same fixed bed reactor as used for activity tests. Aging was conducted isothermally (at 500, 600 or 700 °C) at a space velocity of 12,000 h^{-1} and using a wide time range (15 min to 16 h). After aging, if necessary, the temperature was decreased to 500 °C under nitrogen flow in order to start the reductive pre-treatment of the catalyst followed by the activity test. The aging gas composition was 7% O_2 in nitrogen.

2.4. Microscopic analysis of platinum particles

The particles of platinum were observed by transmission electron microscopy using a Topcon 002B microscope operating at 200 kV. Pictures were taken either before aging of the catalyst or after the aging procedure. Typically, for all samples, the sizes of over 200 Pt particles were measured on the TEM pictures. The software Image J was used to analyze the images in order to obtain the particle size distributions. Platinum particles smaller that 0.5 nm in diameter were not detectable.

3. Results

3.1. Microscopic analysis

3.1.1. Effect of aging duration

The platinum particle size distribution of the fresh 1.6% Pt/Al_2O_3 catalyst is mainly composed of very small particles in the 1–2.5 nm range (Figs. 1(a) and 2). The metal dispersion is calculated from the Pt particle size distribution obtained from TEM measurements by the following equation, assuming spherical particles:

$$D = \frac{6M_{Pt}}{\sigma \rho_{Pt}} \left(\frac{\sum_i n_i d_i^2}{\sum_i n_i d_i^3} \right) \quad (1)$$

where M_{Pt} and ρ_{Pt} are the molar mass and density of Pt, respectively; n_i is the fraction of particles with a diameter d_i, σ is the area occupied by 1 mol of Pt at the surface (3.75×10^4 m^2/mol). The global Pt dispersion is 74%. The same equation as above is obtained if half spheres, with the flat

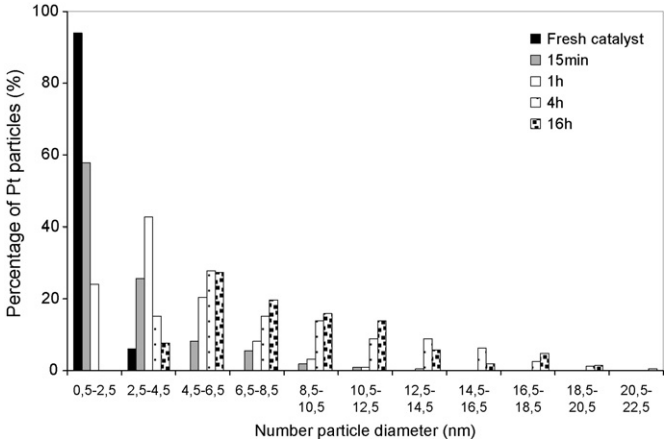

Fig. 2. Effect of the aging duration on the size distribution of the platinum particles. Aging under 7% O_2 at 600 °C.

area in contact with the support are assumed. In the literature, dispersion is generally obtained from CO or H_2 chemisorption, and necessitates a hypothesis about the number of adsorbed molecules per platinum atom.

No modification of the particle diameters is detected after aging of the catalyst under a 7% O_2 in N_2 flow at 500 °C for 20 h. However, after aging at 600 °C for 15 min, the size distribution of the Pt particles shifts towards larger diameters (Figs. 1(b) and 2), indicating sintering of platinum particles. After this aging treatment, 26% of particles have a diameter ranging from 2.5 to 4.5 nm and the overall metal dispersion falls down to 25%. Figs. 1(c) and 2 show that sintering is enhanced when aging duration increases from 1 to 4 h. However, the size distributions of Pt particles obtained after 4 and 16 h of aging at 600 °C are very close (Fig. 2), meaning that the sintering phenomenon is more pronounced during the first 4 h. After 16 h of aging at 600 °C, 35% of Pt particles have a diameter ranging from 2.5 to 6.5 nm, and 65% of Pt particles have a diameter higher than 6.5 nm. The overall metal dispersion is equal to 13%.

The observed increase of sintering with duration of treatment is in agreement with the results of Ruckenstein and Malhotra [7].

3.1.2. Effect of aging temperature

Fig. 3 shows the effect of aging temperature on size distribution of platinum particles obtained by TEM. The sintering effect for an aging time of treatment is enhanced when the aging temperature is increased. Indeed, after 15 min aging at 600 °C, 82% of particles have a diameter smaller than 4.5 nm, this percentage falls down to 52% after aging at 700 °C (Fig. 3). It is observed that sintering of Pt particles is a fast phenomenon. Beyond 15 min of aging at 700 °C, the size distribution of the Pt particles is close to that obtained after 16 h of aging at 600 °C, with a Pt dispersion equal to 12%.

The number average particle diameter d_n and the surface average diameter d_s, defined by

$$d_n = \frac{\sum_i n_i d_i}{\sum_i n_i}, \quad d_s = \frac{\sum_i s_i d_i}{\sum_i s_i}, \quad \text{or} \quad d_s = \frac{\sum_i n_i d_i^3}{\sum_i n_i d_i^2}$$

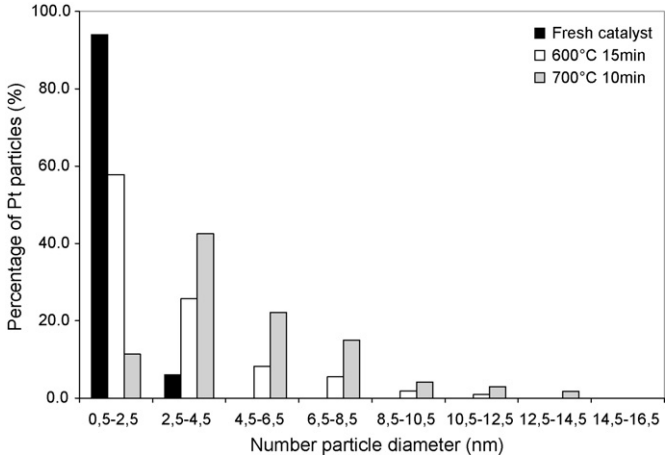

Fig. 3. Effect of the aging temperature on the size distribution of platinum particles. Aging under 7% O_2 during 15 min (600 °C) and 10 min (700 °C).

Table 1
Number (d_n) and surface (d_s) average particle diameters and global metal dispersions D calculated from Eq. (1) for the fresh and aged catalysts

	D (%)	d_n (Å)	d_s (Å)
Fresh catalyst	71	12.5	20.6
T (°C) Duration	D (%)	d_n (Å)	d_s (Å)
Aged catalyst under 7% O_2			
350 2 h	nd	nd	nd
350 20 h	nd	nd	nd
500 20 h	nd	nd	nd
600 15 min	25	30.3	57.7
600 1 h	23	40.8	62.4
600 4 h	12	85.8	122
600 16 h	11	89.3	128
700 10 min	19	49.4	76.8

are given for the fresh and aged materials in Table 1 together with the dispersion D calculated by Eq. (1). Fig. 4 presents the number average particle diameter vs the overall metal dispersion obtained from TEM analysis for the different materials obtained after aging the catalyst under different conditions. As observed, results obtained in the present study agree very well with those obtained by White et al. [28] or Spenadel and Boudart [29] who proposed the following correlation between particle diameter, d_n, and metal dispersion, D: $d_n = 846/D$.

3.2. Activity for CO oxidation measurements

3.2.1. Fresh catalyst

All the results obtained with the fresh catalyst will be used as references to study the effect of catalyst aging on activity. The extent of CO conversion during CO oxidation is plotted vs temperature for the fresh catalyst under different conditions (Fig. 5). From these experiments, the light-off temperature (LOT) is determined as the temperature corresponding to 50% CO conversion in stoichiometric or lean inlet gas composition. When inlet CO is in excess, the LOT is taken as the temperature corresponding to 50% of the maximum CO conversion. In the following discussion, differences larger than 10 °C in the LOT

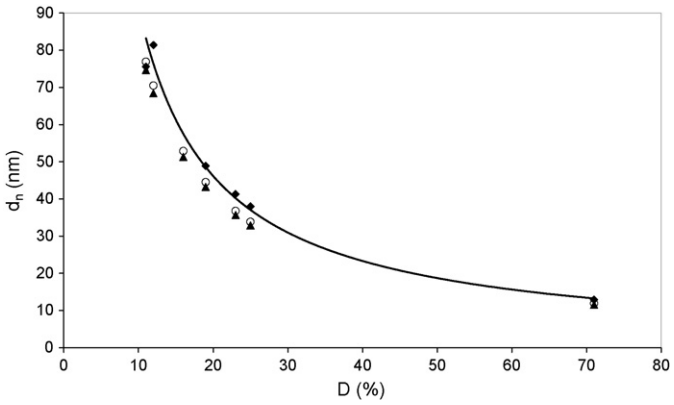

Fig. 4. Number average particle diameter (d_n) as a function of the global metal dispersion (D). (◆) Results presented in the present study, (○) White et al. [28], (▲) Spenadel and Boudart [29].

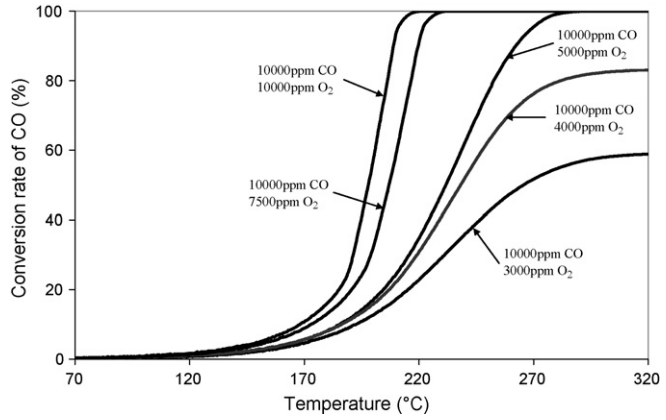

Fig. 5. Extent of CO conversions vs temperature during experiments under a temperature ramp for the fresh catalyst under different inlet gas compositions.

Table 3
CO conversions obtained during steady state isothermal CO oxidations on the fresh catalyst under different inlet gas compositions

CO inlet (ppm)	O_2 inlet (ppm)	τ (%), T_1 = 182 °C	τ (%), T_2 = 166 °C	τ (%), T_3 = 158.5 °C
10,000	3,009	5.9		
10,000	3,997	6.9		
10,000	4,982	8.2		
10,000	7,489	11.0		
10,000	9,997	14.0		
3,000	2,500		nd	14.5
4,000	2,466		16.7	9.0
5,000	2,432		10.7	6.5
6,000	2,412		8.3	4.8
7,000	2,384		6.3	nd

may be regarded as statistically significant. The LOT is given in Table 2. The CO conversion levels obtained under these various conditions with respect to oxygen and CO are reported in Table 3 and will be used to estimate the CO reaction orders.

3.2.2. Aged catalyst

In Fig. 6, the CO conversions under stoichiometric oxidising conditions (10,000 ppm CO and 5000 ppm O_2) for the fresh catalyst and for the catalyst aged at 600 or 700 °C under 7% O_2 during 15 min, 1 h, 4 h or 16 h are compared. The same experiments were carried out under two other inlet gas compositions: 10,000 ppm CO + 3000 ppm O_2, and 4000 ppm CO + 2500 ppm O_2. The corresponding curves are not shown in the present paper.

The light-off temperature differences (ΔT) between the fresh and aged catalysts are listed in Table 4 for the different aging treatments. Clearly, a relation appears between the aging duration and the loss of catalyst activity. When aging is performed at 350 or 500 °C, no effect on the activity is visible, even when the catalyst is aged during 20 h. For such aging treatments, TEM measurements (Section 3.1.1) reveal no particle sintering. For the catalysts aged at 600 °C, the light-off temperature increases with aging duration. Under the stoichiometric conditions, light-off temperature differences (ΔT), between aged and fresh catalyst, increase from 15 °C for an aging duration of 15 min to 48 °C for an aging duration of 16 h. When the catalyst is aged 10 min at 700 °C, the LOT increases by 20 °C. The same trend is observed under the two other reaction conditions. This progressive deactivation of the catalyst during aging, affected by the aging temperature is certainly correlated to the growth of Pt particles observed by TEM. This result was already pointed out by Gracia et al. [16].

However, this effect is complex since during sintering the specific surface of platinum particles decreases, having a negative effect on the catalytic activity. Moreover, the catalytic activity of a Pt particle may also change with the increase of the particle size. From the literature [14–16,19], this structure effect corresponds to an increase of the intrinsic catalytic activity when sintering occurs. Thus, two opposite effects have to be accounted for: on the one hand, the catalytic activity of a platinum particle tends to decrease with the loss of specific surface area and on the other hand, the intrinsic activity increases. Modeling will help to confirm and quantify this second effect.

Table 2
Light-off temperatures for CO oxidation on the fresh catalyst under different inlet gas compositions

CO inlet (ppm)			10,000		
O_2 inlet (ppm)	3,000	4,000	5,000	7,500	10,000
LOT (°C)	266	238	230	207	198

Table 4
Light-off temperature differences between fresh and aged catalysts for the different activity tests

Aging temperature (°C)	Duration	ΔT_{LO} (°C), 10,000 ppm CO/5000 ppm O_2	ΔT_{LO} (°C), 10,000 ppm CO/3000 ppm O_2	ΔT_{LO} (°C), 4000 ppm CO/2500 ppm O_2
350	2 h	–	–	–
	20 h	–	–	–
500	20 h	–	–	–
600	15 min	15	6	9
	1 h	26	16	20
	4 h	38	26	32
	16 h	48	45	44
700	15 min	20	3	4

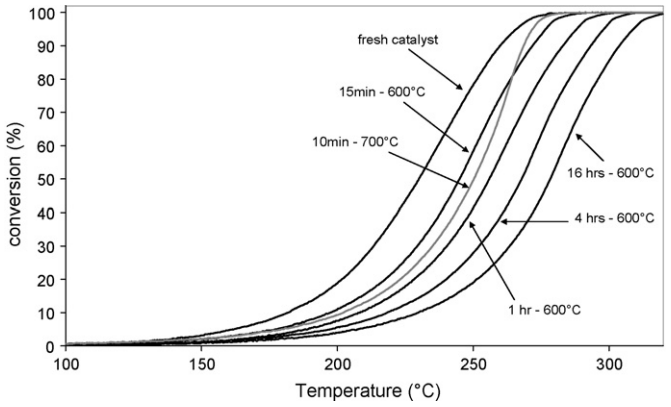

Fig. 6. Extent of CO conversion vs temperature during a temperature ramp for the fresh and aged catalysts at 600 or 700 °C under 7% O_2 during 10 min, 15 min, 1 h, 4 h or 16 h. (CO inlet: 10,000 ppm, O_2 inlet: 5000 ppm).

4. Modeling and discussion

First, the CO conversions as a function of temperature for the fresh catalyst are simulated. Numerous studies try to identify the mechanism for catalytic CO oxidation. This mechanism is still debated. In a recent paper Salomons et al. [30] examined critically the different mechanisms proposed in the literature. Both Eley-Rideal (ER) and Langmuir-Hinshelwood (LH) mechanisms are proposed. The former one was favored in early work while the latter one is currently preferred [32]. The use of a LH mechanism involves reaction orders with respect to CO and O_2 equal to −1 and 1, respectively. However, some authors [31–35] point out that such a simple mechanism is not well suited to modeling the reaction over a wide range of operating conditions. In order to explain all the complex CO oxidation behaviours experimentally observed, few attempts of modifications of the LH model were proposed. Chatterjee et al. [31] used a variation of the LH model considering all steps as reversible. Other authors [33,34,45] introduced an Eley-Rideal reaction (gas phase CO reacting with adsorbed oxygen) together with a LH mechanism. Herz and Marin [33] proposed exclusion models while Engel and Ertl [34] proposed a compressed oxygen model (see refs. [33] and [34] for more details about these mechanisms). Introduction of such variations of the LH mechanism returns a reaction rate with partial reaction orders.

In front of a very complex situation and since in this paper a large range of experimental conditions are examined, only a global kinetic law is established in agreement with all the experimental results. The CO oxidation model has to account for the particle size distribution and its change during the material aging. This makes possible the link between sintering of platinum and the catalytic activity for CO oxidation.

4.1. Modeling of the activity of the fresh catalyst

4.1.1. Reaction rates

The global kinetic law defining the reaction rate r, per surface unit of the platinum particles, is defined by

$$r = k[O_2]^{\alpha}[CO]^{\beta} \tag{2}$$

As TEM measurements revealed that the fresh catalyst is mainly composed of very small particles in the 1–2.5 nm range (Fig. 2), one may consider that the intrinsic catalytic activity of the different Pt particles in the fresh catalyst is the same. From relation (2), the local volumic reaction rate v which represents the number of CO moles consumed per volume unit of the catalytic bed and per second is calculated. Since different classes of particles were identified by TEM, each class (i) contributes to v by

$$v_i(\mathrm{mol_{CO}\,m^{-3}\,s^{-1}}) = r\frac{\rho_{\mathrm{bed}}}{\rho_{\mathrm{Pt}}}\frac{m_{\mathrm{cata}}}{m_{\mathrm{bed}}}6\frac{\tau_{\mathrm{Pt},i}}{d_i} \tag{3}$$

leading to

$$v\,(\mathrm{mol_{CO}\,m^{-3}\,s^{-1}}) = \sum v_i = r\frac{\rho_{\mathrm{bed}}}{\rho_{\mathrm{Pt}\rightleftarrows}}\frac{m_{\mathrm{cata}}}{m_{\mathrm{bed}}}6\sum_i\left(\frac{\tau_{\mathrm{Pt},i}}{d_i}\right) \tag{4}$$

If the reactor operates under differential conditions, CO oxidation rate over the whole bed is expressed by

$$V\,(\mathrm{mol_{CO}\,s^{-1}}) = k[O_2]_0^{\alpha}[CO]_0^{\beta}\frac{m_{\mathrm{cata}}}{\rho_{\mathrm{Pt}}}6\sum_i\left(\frac{\tau_{\mathrm{Pt},i}}{d_i}\right) \tag{5}$$

Using the overall metal dispersion, D, one obtains:

$$V(\mathrm{mol_{CO}\,s^{-1}}) = k[O_2]_0^{\alpha}[CO]_0^{\beta}\frac{m_{\mathrm{cata}}\sigma}{M_{\mathrm{Pt}}}\tau_{\mathrm{Pt}}D \tag{6}$$

The conversion rate, under differential conditions, can also be written using the average surface diameter.

$$V(\mathrm{mol_{CO}\,s^{-1}}) = 6k[O_2]_0^{\alpha}[CO]_0^{\beta}\frac{m_{\mathrm{cata}}}{\rho_{\mathrm{Pt}}}\frac{\tau_{\mathrm{Pt}}}{\overline{d_s}} \tag{7}$$

4.1.2. Determination of the reaction orders

The oxidation rate V is related to the conversion τ as follows:

$$V(\mathrm{mol_{CO}\,s^{-1}}) = \frac{\tau(X_{CO})_0F}{V_m}. \tag{8}$$

Under differential conditions one obtains:

$$\tau = \frac{k}{F}V_m^{1-\alpha-\beta}(X_{\mathrm{co}})_0^{\beta-1}(X_{O_2})_0^{\alpha}\frac{m_{\mathrm{cata}}}{\rho_{\mathrm{Pt}}}6\sum_i\left(\frac{\tau_{\mathrm{Pt},i}}{d_i}\right) \tag{9}$$

Using the experimental results obtained under differential conditions at a given temperature (Table 3), the following values of α and β are thus obtained:

$$\alpha = 0.74, \quad \beta = -0.50$$

These reaction orders highlight the inhibition effect of CO on the rate of reaction. The values of α and β are compared to those obtained by Nicholas and Shah [36] $\beta = -0.28$, $\alpha = 1.07$ and Shishu and Kowalczyk [37] $\beta = -0.5$, $\alpha = 1.0$, using a global model. As expected, these values differ from those usually adopted using of a Langmuir-Hinshelwood model. Nevertheless, Nicholas and Shah [36], who compared kinetic data obtained by the global model and a Langmuir-Hinshelwood dual site model, revealed that both models correlated well

with the experimental data obtained by varying O_2 and CO concentrations from 0.2 to 2.0 mol%.

4.1.3. Determination of the kinetic constant k

From experiments performed under a temperature ramp (Fig. 5), Eq. (9) was used to calculate the experimental values of the kinetic constant k at different temperatures for which the reactor operated under differential conditions ($\tau < 15\%$). The plot of $\ln(k)$ vs $1/T$ leads to the determination of k using an Arrhenius type of function:

$$k(\mathrm{mol}^{0.76}\mathrm{m}^{-1.28}\mathrm{s}^{-1}) = 30\exp\left(-\frac{62,000}{RT}\right) \quad (10)$$

The activation energy E_a obtained (62 kJ/mol) falls within the range of reported values in the literature. Nicholas and Shah [36] proposed an activation energy equal to 27 kJ/mol, using a global model to interpret experiments performed on a 0.27% Pt porous fiber glass catalyst, in a wide range of gas compositions (O_2 and CO concentrations both varying from 0.2 to 2.0 mol%). Shishu and Kowalczyk [37] using an honeycomb platinum catalyst reported a value equal to 66 kJ/mol. Chatterjee et al. [31] using a more restricted range of gas compositions (CO concentration equal to 1.42 vol% and O_2 concentration varying from 0.4 to 1.6 vol%) and a modified Langmuir-Hinshelwood model proposed an activation energy equal to 108 kJ/mol for the surface reaction between moleculary chemisorbed CO and dissociatively chemisorbed oxygen. This last value is close to those obtained by Nibbelke et al. [32] and Gracia et al. [16] who proposed, in a global model, activation energy equal to 112 and 92 kJ/mol, respectively. The broad range of reported literature values of E_a comes from the different experimental conditions used such as the inlet gas composition (stoichiometric, rich or lean mixture), reaction temperature and the initial oxidation state of Pt. Some authors [31,33,38] proposed also a dependence of the activation energy on the surface covered by CO species.

In this study, a wide range of experimental conditions (see Sections 2.2 and 2.3) were used and one demonstrates that a global kinetic law allows a good agreement between theoretical and experimental CO oxidation rates. Thus, it seems to be difficult to compare the value of the obtained activation energy (62 kJ/mol) with those proposed in the literature for other concentration domains. However, it is coherent that our value falls within the range of reported values.

4.1.4. Modeling of the complete oxidation curves during a temperature ramp

Considering the overall CO conversion curves measured during a temperature ramp, X_{CO} and X_{O_2} are not uniform along the catalytic bed thickness. Assuming a quasi steady-state regime one obtains the two following differential equations:

$$\frac{\partial X_{CO}}{\partial z} + C_1 k X_{O_2}^{\alpha} X_{CO}^{\beta} = 0 \quad (11)$$

$$\frac{\partial X_{O_2}}{\partial z} + \frac{C_1}{2} k X_{O_2}^{\alpha} X_{CO}^{\beta} = 0 \quad (12)$$

with

$$C_1 = \frac{6}{d_n}\frac{\rho_{bed}}{\rho_{Pt}}\frac{m_{cata}}{m_{bed}}\tau_{Pt}\frac{S}{F}V_m^{1-\alpha-\beta}$$

$(= 3.2 \times 10^5\ \mathrm{mol}^{-0.76}\ \mathrm{m}^{0.28}\ \mathrm{s}$ in the present conditions).

These equations associated to the boundary conditions: at $z = 0$, $X_{CO} = (X_{CO})_0$ and $X_{O_2} = (X_{O_2})_0$ control the molar fractions of CO and O_2 along the thickness of the catalytic bed.

Moreover, from the stoichiometric of the CO oxidation reaction, the two terms X_{CO} and X_{O_2} are related as expressed below:

$$(X_{O_2})_z = \frac{1}{2}(X_{CO})_z - \left[\frac{(X_{CO})_0}{2} - (X_{O_2})_0\right]. \quad (13)$$

Combining Eqs. (11)–(13) one obtains:

$$\frac{\partial X_{CO}}{\partial z} + C_1 k\left\{\frac{1}{2}X_{CO} - \left[\frac{(X_{CO})_0}{2} - (X_{O_2})_0\right]\right\}^{\alpha} X_{CO}^{\beta} = 0 \quad (14)$$

This equation is solved numerically by the Euler method in which the previously determine value of k (Eq. (10)) is used.

Fig. 7 compares the experimental CO conversion curves with the calculated ones thus obtained. As shown, a fair agreement is obtained between the experimental CO conversion curve and the calculated one. However, at a temperature above 240 °C in excess of CO (Fig. 7b) or under stoichiometry (Fig. 7c) a slight discrepancy occurs. This discrepancy appears when the CO conversion rate is high, making difficult a precise measure of the CO_2 molar fraction.

4.2. Modeling of the activity of the catalysts after sintering (aged catalysts)

By using the previously determined value of k for the fresh catalyst one obtains an underestimation of the CO conversion for the aged catalyst, whatever the temperature, although the surface area of platinum after sintering was accounted for. Two main assumptions could by proposed to explain this result:

(a) The occurrence of a metal–support interaction. As a function of pre-treatment conditions, the genesis of a strong metal–support interaction (SMSI) may occur on some noble supported metals [39–46]. This phenomenon induces modification of the metal–support interface and then affects the catalytic activity of noble metals. This was highlighted with noble metals impregnated on reducible supports such as TiO_2, ZrO_2 or ceria [39–45]. The SMSI depends on reduction temperature of the catalyst during pre-treatment. Two main explanations are given in the literature to explain metal–support interaction according to the reduction temperature: (i) $T_{red} < 500$ °C: pure electronic interactions due to oxygen vacancies allowing the presence of quasi-free electrons contributing to electronic enrichment of the noble metal and special sites at the metal–support interface [39,44,45] or (ii) $T_{red} > 500$ °C: migration and then decoration or encapsulation of the metal by partly reduced support species leading to the decrease of the

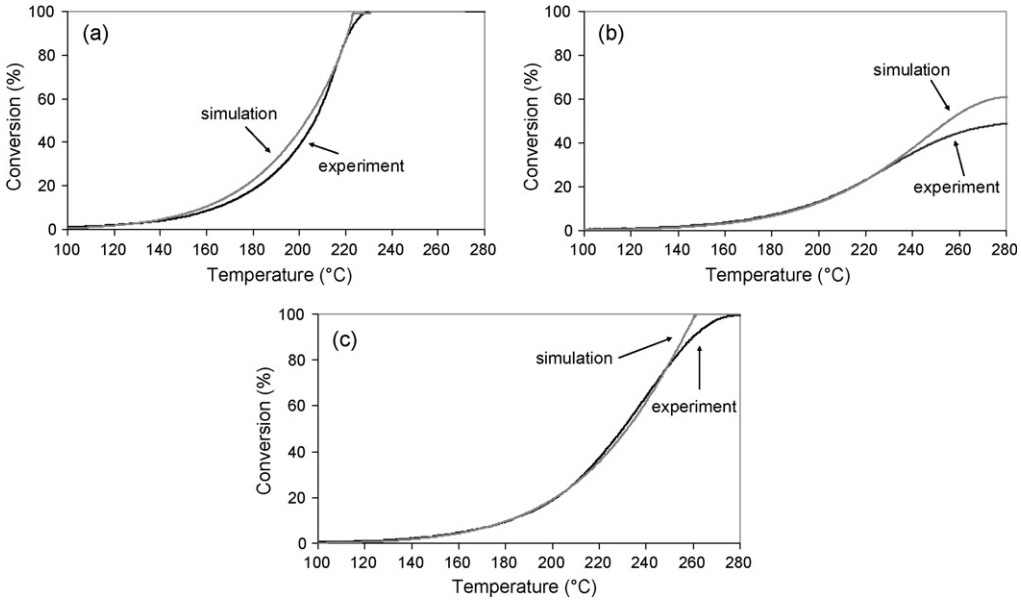

Fig. 7. Comparison of the experimental CO conversion curves and the calculated ones for the fresh 1.6% Pt/Al_2O_3 catalyst using the following kinetic constant: $k = 30\exp(-62{,}000/RT)$. Experimental conditions: (a) $(X_{CO})_0 = 4000$ ppm; $(X_{O_2})_0 = 2500$ ppm. (b) $(X_{CO})_0 = 10{,}000$ ppm; $(X_{O_2})_0 = 3000$ ppm. (c) $(X_{CO})_0 = 10{,}000$ ppm; $(X_{O_2})_0 = 5000$ ppm.

accessible metallic surface [39–42]. Although, SMSI was mainly observed after reduced pre-treatment, Fan et al. [46] suggested that calcinations in air at 1050 °C of a 2% Pt/CeO_2-ZrO_2 catalyst lead to encapsulation of Pt particles by ceria. On the other hand, these authors attribute the increase of catalytic performances towards NO, CO and C_3H_8 oxidation, with increasing calcination temperature from 500 to 900 °C, to an increase of oxygen vacancies.

(b) CO/O_2 reaction is structure sensitive meaning that k is affected by the particle size. The structure sensitivity of CO/O_2 reaction is a long-debated issue. Under stoichiometric or CO-rich conditions, CO oxidation was found to be not structure sensitive on large Pt particles (>2.5 nm) [20–27]. On the other hand, for small particles (between 1 and 4 nm) CO/O_2 reaction is reported to be structure sensitive whatever the inlet CO/O_2 ratio [14–19].

In order to quantify the structure effect, a relationship between the rate constant k_i and the particle diameter d_i has to be taken into account. Szabo et al. [47] and Sierra et al. [48] found, on single crystals, that CO oxidation on metallic plane surface is faster than on step sites. This result was recently confirmed by Gracia et al. [16], using catalysts containing 2% wt Pt on silica with different metal dispersions (29–76%) corresponding to a mean particle diameter in the range 13.5–51.1 Å. Kinetic studies revealed that the turn over frequency of CO oxidation increases with increasing Pt particle size [16]. To explain that the catalytic activity depends on the particle size, Gracia et al. [16] considered in their Monte Carlo simulation a model of a Pt crystallite depicted in Fig. 8 of ref. [16]. In their simulations, these authors assume that different catalytic sites with different reactivities are at work with the fractions of these different sites depending on the particle size. As the crystallite size increases, the fraction of Pt atoms on corners and edges decreases while the fraction of atoms on planer faces increases. Using this simulation, these authors found that the experimental rates only agree with the theory when the rate of surface reaction on corners and edges is at least 10 times smaller than that on planar faces. However, no kinetic data are given by these authors.

In the present study an inert support was used, excluding the formation of special sites at the metal–support interface due to oxygen vacancies formed during aging treatment. Moreover, one may consider that encapsulation of Pt particles by the support, if occurring, is already taken into account in the calculation of the metal dispersion from TEM measurement (Eq. (6)). Consequently, one may assume that the increase of CO oxidation rate obtained after sintering is probably due to a structure effect with the kinetic constant k_i increasing with the particle diameter.

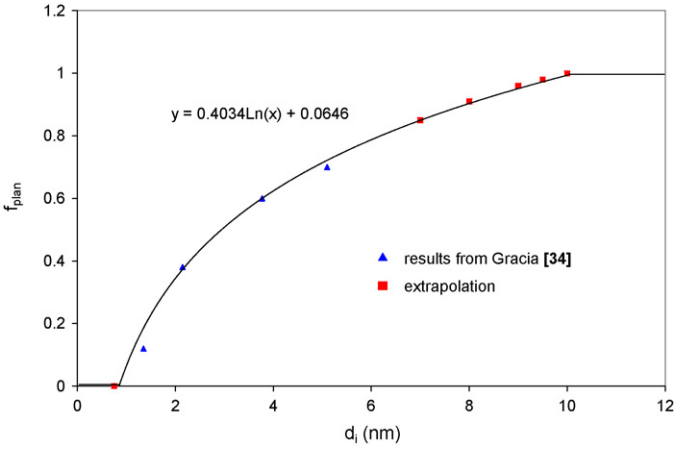

Fig. 8. Relation between fraction of atoms in planar faces and particles diameter.

For simplicity, only two groups of platinum atoms are considered to quantify this structure effect. The first one consists in atoms in planar faces and the second one includes all other types of atoms especially those located on edges and corners. The fractions of atoms belonging to each group are named f_{plan} and f_{other}, respectively. ($f_{plan} + f_{other} = 1$). Gracia et al. [16] established the following equation for particle sizes in the range 13.5–51.1 Å (see Fig. 8):

$$f_{plan(d_i)} = 0.4034 \ln(d_i) + 8.4247 \quad (15)$$

This equation is assumed by extrapolation to apply for the present particle size range, i.e., from 0.75 to 10 nm. It is assumed that under 0.75 nm f_{plan} is equal to 0 and above 10 nm f_{plan} is equal to 1.

Accordingly, two intrinsic kinetic constants, k_{plan} and k_{other}, corresponding to the intrinsic reactivity of both groups of atoms are considered.

Thus, the kinetic constant k_i related to particles having a diameter equal to d_i may be written as follows:

$$k_i = f_{plan(d_i)} k_{plan} + f_{other(d_i)} k_{other} \quad (16)$$

The rate of CO oxidation is higher on atoms located on planar faces. The reason proposed by Gracia et al. [16] is that CO molecules adsorbed at corner and edge sites, which are low coordination platinum atoms, have to overcome an additional barrier energy to diffuse and react, decreasing the rate of surface reaction. Since the fraction of planar atoms increases with d_i, a higher reaction rate is obtained for larger particles.

Considering a constant value for the ratio (k_{plan}/k_{other}), whatever the temperature it comes:

$$\frac{k_{plan}}{k_{other}} = a, \quad a \text{ being a constant} > 1 \quad (17)$$

This hypothesis implicitly imposes that the activation energies are the same for the reactions occurring on planar regions and other regions. There are no fundamental reasons for that. Considering two different activation energies E_{other} and E_{plan}, (k_{plan}/k_{other}) writes $\frac{k_{plan}}{k_{other}} = \frac{A_{plan}}{A_{other}} \exp\left(\frac{1}{RT}(E_{other} - E_{plan})\right)$

If ($E_{other} - E_{plan}$) remains small (this is probably the case) compared to E_{other} (or E_{plan}), (k_{plan}/k_{other}) approximates to a constant. One could introduce in the model a value for ($E_{other} - E_{plan}$) and another one for (A_{plan}/A_{other}) (the ratio of the pre-exponential factors). This should be more realistic but should necessitate to adjust the values of two parameters. This fitting procedure should lead to different couples of values for ($E_{other} - E_{plan}$) and (A_{plan}/A_{other}) with the difficulty to identify the right couple. For this reason, we keep simplicity for the model since, up to now, no theoretical indications can help to choose between the different couples.

According to Eqs. (16) and (17) one obtains:

$$k = k_{plan}\left[\left(1 - \frac{1}{a}\right) f_{plan(d_i)} + \frac{1}{a}\right] \quad (18)$$

in which the two parameters k_{plan} and a have to be determined.

The rate constant k_i depending on the particle size, Eq. (5) becomes:

$$V = [O_2]_0^{\alpha}[CO]_0^{\beta} \frac{m_{cata}}{\rho_{Pt}} 6 \sum\left(\frac{\tau_{Pt,i} k_i}{d_i}\right) \quad (19)$$

This equation should apply to all types of experimental conditions (different volumic fractions of CO and O_2) for fresh and aged catalyst samples assuming differential reactor conditions.

Knowing the value of V from experiments one determines the value of $\sum k_i \tau_i / d_i$ at 180 °C. At this temperature and for a given aged sample, this term should be a constant whatever the gas composition. Indeed, it was verified that for different gas compositions the value of $\sum k_i \tau_i / d_i$ is constant since less than 5% of fluctuation is observed.

According to Eq. (18), this term writes

$$\sum\left(\frac{\tau_i k_i}{d_i}\right) = k_{plan} \sum\left\{\frac{\tau_i}{d_i}\left[\left(1 - \frac{1}{a}\right) f_{plan(d_i)} + \frac{1}{a}\right]\right\} \quad (20)$$

According to the used hypotheses, k_{plan} should be, at a given temperature, a constant for all samples since it corresponds to the intrinsic activity of Pt located on the planar faces. Hence, the value of the rate constant k_{plan} may be calculated from Eq. (20) when having the value of a. Therefore, the value of a is varied between 1 and 10 for the different aged samples in order to calculate k_{plan}. The value of k_{plan} is expected to be a constant. This procedure leads to estimate the best value of a which leads to the less dispersed values of k_{plan}. This value is equal to 2.5. Using this 2.5 value, k_{plan} is found to be 3.8×10^6 mol$^{0.76}$ m$^{-1.28}$ s^{-1} with a variance equal to 0.3×10^6. Using this procedure at a temperature between 180 and 200 °C, one obtains the following equation reflecting the change of k_{plan} with temperature:

$$k_{plan} = 103 \exp\left(-\frac{64,500}{RT}\right). \quad (21)$$

Combining Eqs. (14) and (18) one obtains:

$$\frac{\partial X_{CO}}{\partial z} + C_2 k_{plan} \sum_i \left\{\frac{\tau_{Pt,i}}{d_i}\left[\left(1 - \frac{1}{a}\right) f_{plan(d_i)} + \frac{1}{a}\right]\right\}\left\{\frac{1}{2} X_{CO} - \left[\frac{(X_{CO})_0}{2} - (X_{O_2})_0\right]\right\}^{\alpha} X_{CO}^{\beta} = 0 \quad (22)$$

with

$$C_2 = 6 \frac{\rho_{lit}}{\rho_{Pt}} \frac{m_{cata}}{m_{lit}} \frac{S}{D_T} V_m^{1-\alpha-\beta}$$

Then, CO oxidation runs under different conditions (different CO and O_2 molar fractions), during a temperature ramp, are simulated using Eq. (22) and using the previously defined (Section 4.1.4) numerical procedure and calculated values of α and β. Examples of a satisfactory agreement between experimental and computed conversion curves are given in Fig. 9. The larger deviations are obtained for the materials aged at 600 °C during 15 min (Fig. 9a) and at 700 °C during 1 h (Fig. 9b). These deviations occur at temperatures

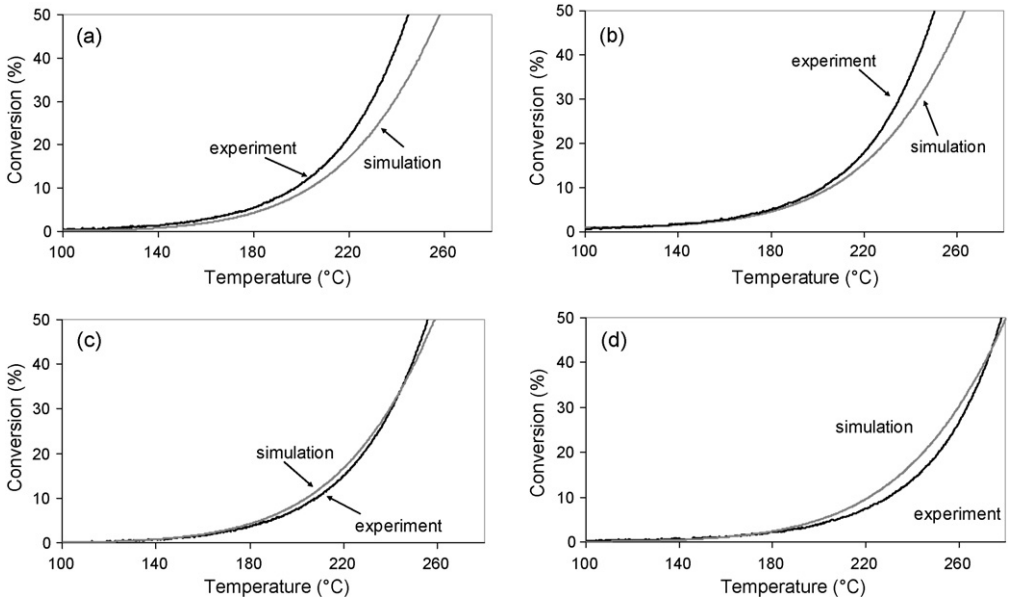

Fig. 9. Comparison of the experimental CO conversion curves and the calculated ones for aged 1.6% Pt/Al_2O_3 catalysts using the following kinetic constant: $k_{plan} = 103 \exp(-65{,}400/RT)$ and $k_{other} = (1/a)k_{plan}$. Experimental conditions: $(X_{CO})_0 = 10{,}000$ ppm; $(X_{O_2})_0 = 5000$ ppm. Aging conditions under 7% O_2/N_2: (a) 600 °C during 15 min, (b) 700 °C during 10 min, (c) 600 °C during 1 h, (d) 600 °C during 16 h.

above the temperature domain used for the determination of a. A perfect agreement is found for the fresh catalyst (see Fig. 10 for $a = 2.5$).

It is important to assess how much the determined value of a affects the predicted CO conversion curve. This was done in Fig. 10 by modeling CO conversion on the fresh catalyst with different a values (1, 2.5, 5 and 10). The value $a = 1$ means that there is no structure effect ($k_{plan} = k_{other}$). The experimental CO conversion curve is also plotted. The strong influence of the value of a is obvious up to $a = 5$. For $a > 5$, the contribution of the platinum atoms which are not located in planar faces becomes negligible, causing a decrease of the structure effect.

For the aged materials, the effect of the value of a becomes much smaller since few particles have a diameter smaller than 10 nm. For $d_i > 10$ nm, the kinetic constant k_i does not depend on the diameter according to the proposed law (Eq. (17)). This means that the fresh catalyst is the most adequate material for estimating the value of a.

It is interesting to note that for two different samples for which the value of $\sum \tau_i/d_i$ are very close, one observes that the CO conversion curves are also very close. For example, for the catalysts aged during 15 min or 1 h, the corresponding values of $\sum \tau_i/d_i$ are very close (shift of 7.3% corresponding to 2.6×10^6 for 1 h aging and 2.4×10^6 for 15 min aging). This means that the value of the term $\sum \tau_i/d_i$ plays a very important role in the catalytic activity of the material. This demonstrates that the surface average diameter, d_s ($\sum_i(\tau_i/d_i) = (\tau_{Pt}/d_s)$) is a key parameter for the catalytic activity of the material. However, it is seen in Eq. (22) that the term controlling the reactivity is not $\sum \tau_i/d_i$ but $\sum k_i\tau_i/d_i$. In fact, one observes that when two ratios $\sum \tau_i/d_i$ are close, the two ratios $\sum k_i\tau_i/d_i$ are also very close.

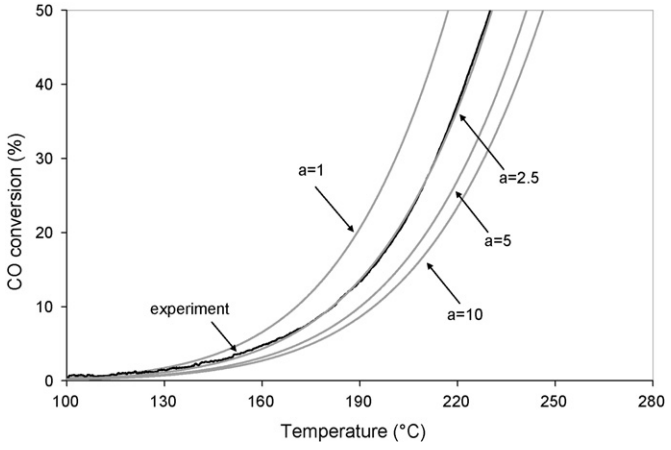

Fig. 10. Effect of the value of a on the CO conversion simulated curves obtained with the fresh catalyst.

5. Conclusion

Aging of a Pt/Al_2O_3 catalyst was performed under different conditions and the size distribution of the platinum particles has been determined by transmission electron microscopy. The fresh catalyst has a particle size distribution in the range 0.5–4.5 nm with 88% in the range 0.5–2.5 nm. The size distribution shifts towards larger diameters when the aging duration increases or when the aging temperature goes up from 600 to 700 °C. At 500 °C, no sintering is observed. The sintering phenomenon is unquestionable but it remains difficult to correctly dispatch all the platinum particles within the different particles diameter classes. However, for the fresh material and all aged samples, it was possible to estimate the dispersion of the distribution based on the measured diameters as well as the number average diameter and the surface average diameter.

The activities of the fresh and the aged catalysts for the CO conversion were studied in a fixed bed reactor. A global kinetic model was proposed, using a fitted kinetic constant given under an Arrhenius form, to simulate the CO conversion on a fresh catalyst during a temperature ramp under different CO and O_2 inlet concentrations. When this model is used to simulate the activity of an aged samples, accounting for the new surface of platinum particles, CO conversion is underestimated. This is the proof of a structure effect with the kinetic constant increasing with the particle diameter. Two intrinsic kinetic constants related to platinum atoms located either in planar faces or on edges and corners are considered. The catalytic activity of platinum sites is assumed to be higher for atoms in plane. A ratio of 2.5 between the kinetic constants defined for atoms in planar faces and the other ones (k_{plan}/k_{other}) allows to obtain a satisfactory agreement between experimental and predicted CO conversion curves for the different aged materials used under different inlet CO and O_2 concentrations.

Acknowledgments

The authors thank the 'Region Alsace' for a research grant for J.Y. and the network REALISE (REseau Alsace de Laboratoire en Ingénierie et Sciences pour l'Environnement) for its financial support for equipment facilities.

References

[1] A.K. Neyestanaki, F. Klingstedt, T. Salmi, D.Y. Murzin, Fuel 83 (2003) 395.
[2] A.K. Datye, Q. Xu, K.C. Kharas, J.M. McCarty, Catal. Today 111 (2006) 59.
[3] P. Lööf, B. Stenbom, H. Norden, B. Kasemo, J. Catal. 144 (1993) 60.
[4] D.J. Smith, D. White, T. Baird, J.R. Fryer, J. Catal. 81 (1983) 107.
[5] C.G. Granqvist, R.A. Buhrman, J. Appl. Phys. 47 (1976) 2200.
[6] H. Bartholomew, Appl. Catal. A 212 (2001) 17.
[7] E. Ruckenstein, M.L. Malhotra, J. Catal. 41 (1976) 303.
[8] A. Bellare, D.B. Dadyburjor, M.J. Kelley, J. Catal. 117 (1989) 78.
[9] P. Wynblatt, N.A. Gjostein, Scr. Metall. 7 (1973) 969.
[10] P. Forzatti, L. Lietti, Catal. Today 52 (1999) 165.
[11] S.E. Wanke, P.C. Flynn, Catal. Rev.-Sci. Eng. 12 (1975) 93.
[12] Y.J. Mergler, B.E. Nieuwenhuys, J. Catal. 161 (1996) 292.
[13] P. Granger, C. Dathy, J.J. Lecomte, L. Leclercq, M. Prigent, G. Mabilon, G. Leclercq, J. Catal. 173 (1998) 304.
[14] G.S. Zafiris, R.J. Gorte, J. Catal. 140 (1993) 418.
[15] E.C. Akubuiro, X.E. Verykios, L. Lesnick, Appl. Catal. B 14 (1985) 215.
[16] F.J. Gracia, L. Bollmann, E.E. Wolf, J.T. Miller, A.J. Kropf, J. Catal. 220 (2003) 382.
[17] H. Matsuhashi, S. Nishiyama, H. Miura, K. Eguchi, K. Hasegawa, Y. Iizuka, A. Igarashi, N. Katada, J. Kobayashi, T. Kubota, Appl. Catal. A 272 (2004) 329.
[18] M. Che, C.O. Bennett, Adv. Catal. 36 (1989) 55.
[19] D.N. Belton, S.J. Schmieg, Surf. Sci. 202 (1988) 238.
[20] E. McCarthy, J. Zahradnik, G.C. Kuczynski, J.J. Carberry, J. Catal. 39 (1975) 29.
[21] L. Kieken, M. Boudart, Stud. Surf. Sci. Catal. 75 (1993) 1313.
[22] S. Ladas, H. Poppa, M. Boudart, Surf. Sci. 102 (1981) 151.
[23] S.H. Oh, C.C. Eickel, J. Catal. 128 (1991) 526.
[24] S.H. Oh, G.B. Fisher, J.E. Carpenter, D.W. Goodman, J. Catal. 100 (1986) 360.
[25] C. Wong, R.W. McCabe, J. Catal. 119 (1989) 47.
[26] N.W. Cant, R.A. Donaldson, J. Catal. 71 (1981) 320.
[27] X. Xu, J. Szanyi, Q. Xu, D.W. Goodman, Catal. Today 21 (1994) 57.
[28] D. White, T. Baird, J.R. Fryer, L.A. Freeman, D.J. Smith, M. Day, J. Catal. 81 (1983) 119.
[29] L. Spenadel, M. Boudart, J. Phys. Chem. 64 (1960) 204.
[30] S. Salomons, R.E. Hayes, M. Votsmeier, A. Drochner, H. Vogel, S. Malmberg, J. Gieshoff, Appl. Catal. B 70 (2007) 305.
[31] D. Chatterjee, O. Deutschmann, J. Warnatz, Faraday Discuss. 119 (2001) 371.
[32] R.H. Nibbelke, M.A.J. Campman, J.H.B. Hoebink, G.B. Marin, J. Catal. 171 (1997) 358.
[33] R.K. Herz, S.P. Marin, J. Catal. 65 (1980) 281.
[34] T. Engel, G. Ertl, Adv. Catal. 28 (1979) 1.
[35] J.M.A. Harmsen, J.H.B. Hoebink, J.C. Schouten, Ind. Eng. Chem. Res. 39 (2000) 599.
[36] D.M. Nicholas, Y.T. Shah, Ind. Eng. Chem. Prod. Res. Dev. 15 (1976) 35.
[37] R.C. Shishu, L.S. Kowalczyk, Platinum Met. Rev. 18 (1974) 58.
[38] M. Rinnemo, D. Kulginov, S. Johnsson, K.L. Wong, V.P. Zhdanov, B. Kasemo, Surf. Sci. 376 (1997) 297.
[39] A. Dandekar, M.A. Vannice, J. Catal. 183 (2) (1999) 344.
[40] L.F. Liotta, A. Longo, A. Martorana, G. Pantaleo, A.M. Venezia, G. Deganello, Appl. Catal. B 48 (2004) 133.
[41] S. Bernal, J.J. Calvino, M.A. Cauqui, J.M. Gatica, C. Larese, J.A. Perez Omil, J.M. Pintado, Catal. Today 50 (1999) 175.
[42] A. Holmgren, F. Azarnoush, E. Fridell, Appl. Catal. B 22 (1999) 49.
[43] G.W. Graham, H.W. Jen, W. Chun, R.W. McCabe, J. Catal. 182 (1999) 228.
[44] J.H. Bitter, M.A. Cauqui, J.M. Gatica, S. Bernal, D.E. Ramaker, D.C. Koningsberger, in: A. Corma, F.V. Melo, S. Mendioroz, J.L. Fierro (Eds.), Stud. Surf. Sci. Catal., Elsevier, Amsterdam, 2000, p. 3183.
[45] D.R. Mullins, K.Z. Zhang, Surf. Sci. 513 (2002) 163.
[46] J. Fan, X. Wu, L. Yang, D. Wenig, Catal. Today 126 (2007) 303.
[47] A. Szabo, M.A. Henderson, J.T. Yates, J. Chem. Phys. 96 (8) (1992) 6191.
[48] J. Sierra, R. Van Silfhout, F. Rutten, B.E. Nieuwenhuys, Stud. Surf. Sci. Catal. 71 (1991) 395.